Introducing Mutual Heating Effects in the Ladder-Type Soil Model for the Dynamic Thermal Rating of Underground Cables

Marc Diaz-Aguiló and Francisco de León, *Fellow, IEEE*

***Abstract*—The proper modeling of the transient thermal behavior of mutual heating effects between underground power cables is very important for the rating of transmission and distribution cables. The IEC standards proposed an accurate model based on exponential integrals that it can be difficult to implement in basic electrical software. The model is not consistent with the layered modeling of the cable thermal resistances. In this paper, a simple and easy-to-use alternative model is presented. It consists of injecting the correct current at the right position of the RC circuit representing the soil. The new model can accurately reproduce the full physics of the transient phenomenon and is consistent with the modeling of the cable used in the IEC standards themselves. The new model is tested and validated against numerous finite-element simulations for realistic cable installations.**

***Index Terms*—Mutual heating, power systems, power system measurement, real-time thermal rating, thermal modeling, underground cables.**

I. Introduction

MODELING the soil correctly is very important for the calculation of the thermal performance of underground power cables. Actually, after the conductor gauge and maybe the bonding technique, the soil thermal resistivity is the factor that limits the ampacity the most in an underground cable system [1], [2]. The IEC and the IEEE standards [3], [4] determine the steady-state thermal rating of cables via an analog-equivalent thermal-electrical circuit.

In recent years, in addition to the steady-state rating, dynamic thermal calculations for emergency ratings are becoming increasingly important [5]–[14]. Better modeling, more advanced grid infrastructure, and faster computation capabilities in the context of smart-grid operations lead to the necessity of determining the real-time ratings of power cables [8], [12]. Also, current research shows that accurate real temperature transients can be used to determine the useful life of cables in service with dedicated life models [15], [16]. This is very important for electric utilities because it directly impacts their asset-management strategy. The real-time thermal rating (RTTR) systems need to very accurately model not only the cable but also the surroundings to deliver accurate and trustworthy results [17]. The majority of the approaches used in RTTR systems use the guidelines of the IEC standards to model transients in underground cables.

For steady calculations, the model of the cable is built from the T_1, T_2, and T_3 equivalent resistances as defined in the IEC standards [3]. The surroundings (soil, duct banks, backfills, ducts, pipes, etc.) are modeled with an equivalent resistance (T_4) [3]. The effects of mutual heating from neighboring cables are precisely included in the model with a simple and easy-to-use formulation based on the image method [3]. An alternative formulation was presented in [18].

In contrast with the simple model used for steady-state ratings in the IEC standards, the same methodology is not used for transient (or dynamic) applications [5]. The effect of soil and the mutual heating effects of neighboring cables is included using the analytical solution of the diffusion equation, requiring the evaluation of exponential integrals and/or the evaluation of the attainment factors [5]. This solution is very precise, but not consistent with the layered *RC* modeling that the standards themselves propose for the cable layers. Also, in [19], an interesting alternative model based on the summation of exponential functions is used to model the cable environment.

This paper proposes that the mutual interaction effects can be properly modeled by injecting the losses of the neighboring cables at specific locations in the *RC* ladder. The model extends the *RC* circuit model representing the soil proposed in [20] and [21] and optimized in [22] to include mutual heating. Therefore, the proposed model is perfectly consistent with the modeling techniques for the cable used in the IEC standards themselves. The new model does not exactly reproduce the IEC solutions but can reproduce accurately the physics of the transient phenomenon for the majority of practical applications. In addition, the model is computationally efficient and allows the use of the powerful analytical tools available for state-space equations, which are based on matrix theory and are a compact form of representing a set of differential equations. The new model is tested and validated against numerous finite-elements simulations for realistic cable installations. The characteristics of this model have been presented in [22], but it is succinctly described in the Appendix of this paper for the sake of completeness.

Easy-to-use and accurate modeling tools are necessary to enable fast and reliable analysis of the thermal behavior of

Manuscript received July 27, 2014; revised October 07, 2014 and December 05, 2014; accepted January 05, 2015. Date of publication January 13, 2015; date of current version July 21, 2015. Paper no. TPWRD-00920-2014.

The authors are with the Department of Electrical and Computer Engineering, New York University, Brooklyn, NY 11201 USA (e-mail: marc.diaz.aguilo@gmail.com; fdeleon@nyu.edu).

Color versions of one or more of the figures in this paper are available online at http://ieeexplore.ieee.org.

Digital Object Identifier 10.1109/TPWRD.2015.2390072

power cables. This would certainly avoid dangerous situations affecting the stability and resiliency of the power grid. The model of this paper can be easily integrated into the available software and models for real-time thermal rating systems that benefit state-space forms in order to use available parameter estimation techniques or recursive filtering [8], [17], [23].

II. Underlying Theory and the IEC Standard

The IEC 60853 standard states that the transient temperature rise of the outer surface of the hottest cable $\theta_e(t)$ for long durations should be computed as [5]

$$\theta_e(t) = \frac{\rho_T W_I}{4\pi} \cdot \left[-E_i\left(\frac{-D^2}{16\delta t}\right) + E_i\left(\frac{-L^2}{\delta t}\right)\right] + \frac{\rho_T W_I}{4\pi} \cdot \sum_{k=1}^{N-1} \left[-E_i\left(\frac{-{d_{pk}}^2}{4\delta t}\right) + E_i\left(\frac{-{d'_{pk}}^2}{4\delta t}\right)\right] \quad (1)$$

where W_I is the total power loss per-unit length of each cable (if they are all equally loaded), d_{pk} is the distance from cable k to the center of cable p, and d'_{pk} is the distance from the image of the center of cable k to the center of cable p, and N is the number of cables in the installation [24]. ρ_T is the thermal resistivity of the soil, E_i is the exponential integral, D is the diameter of the cable, L is the laying depth of the cable, and δ is the soil diffusivity. All of these variables are specified in [5] [Part 2, (4)–(36)]. Equation (1) is the solution of the diffusion equation when representing the cables as line sources and when an isothermal surface is assumed at the soil-air interface. These assumptions lead to the theory of images solved first by Kennelly [25] and later discussed by Neher and McGrath [24], [26]. For short duration transients, the influence of the images can be suppressed in (1). Therefore, (1) can be reduced to

$$\theta_e(t) = \frac{\rho_T W_I}{4\pi} \cdot \left\{ \left[-E_i\left(\frac{-D^2}{16\delta t}\right)\right] + \sum_{k=1}^{k=N-1} \left[-E_i\left(\frac{-{d_{pk}}^2}{4\delta t}\right)\right]\right\}. \quad (2)$$

Also, the summation term in (2) is likely to be negligible for short periods of time unless the cables are touching or are very close to each other [5]. This formulation is specified in [5] (Part 2, 4–70) of the standard. Also, if all cables are not equally loaded, W_I can be substituted for the corresponding losses of each cable. Finally, if $\theta_e(t)$ is combined with the cable model, in 4–71 of the standard, the attainment factors are introduced [5].

This formulation is very precise but it requires the solution of exponential integrals for every time step. The Exponential E_i is not an elementary function. For its evaluation over a wide range of arguments, series expansions are needed. Note though that in the majority of practical cases in cables ampacity, only a few expansion terms are needed for accurate results.

For steady-state conditions, the formulation in [5] can be simplified if (1) is evaluated for $t \to \infty$. In this scenario, the formulation for steady state can be rewritten as

$$\Delta\theta_p = W_p T_4 + \sum_{k=1}^{N-1} W_k \frac{1}{2\pi}\rho_T \ln\left(\frac{d'_{pk}}{d_{pk}}\right) \quad (3)$$

where the total temperature rise at the surface of the cable under analysis $\Delta\theta_p$ is a superposition of the effects caused by the losses in the same cable (W_p) and the losses in the other cables (W_k).

The IEC standards 60287 [3] define these values in steady-state conditions separately, by defining T_4 for a single cable as

$$T_4 = \frac{1}{2\pi}\rho_T \ln(u + \sqrt{u^2 - 1}) \quad (4)$$

and the contribution from all the other cables with an equivalent temperature rise of

$$\Delta\theta_{kp} = \frac{1}{2\pi}\rho_T W_k \ln\left(\frac{d'_{pk}}{d_{pk}}\right) \quad (5)$$

where u is defined as $u = 2L/D$.

These formulations are very precise and easy to use for steady-state calculations of the ampacity of underground cables. However, there is no analog *RC* circuit presented in the IEC or IEEE standards for transient calculations. This paper fills the void.

III. Proposed Model

A model that accurately reproduces (1) for one cable has been reported in [20] and [21] and was optimized in [22]. Essentially, these models suggest that when only one cable is under analysis, the surrounding soil can be modeled with an *RC* electrothermal equivalent ladder circuit; see Fig. 1(a). However, nothing has been found in the literature on how to model the transient evolution of the mutual heating interactions of multiple underground cables.

The mutual interaction effects are properly modeled in this paper by injecting the losses of the neighboring cables at specific locations in the *RC* ladder (see Fig. 1). From Fig. 1(a), one can compute T_4 as follows:

$$T_4 = \sum_{i=0}^{M} \frac{1}{2\pi} R_{si} \quad (6)$$

where R_{si} are the individual thermal resistances of each of the M layers in the ladder-type soil model. As explained in [21] and [22], the values of C_{si} (thermal capacitances) are calculated by also taking into account the geometry of each soil layer that is used to calculate R_{si}. (See the Appendix for further details.) The model can be enhanced if the same framework is used to consider the effects of mutual heating from the neighboring cables. The enhanced model needs to be accurate in steady-state and transient computations.

As was described in the previous section, particularly in (5), the IEC standard models very precisely the temperature rise caused by each neighboring cable k onto the cable under analysis (p) in steady-state conditions. To make (5) consistent with the standard equations that model the inner layers of the cable,

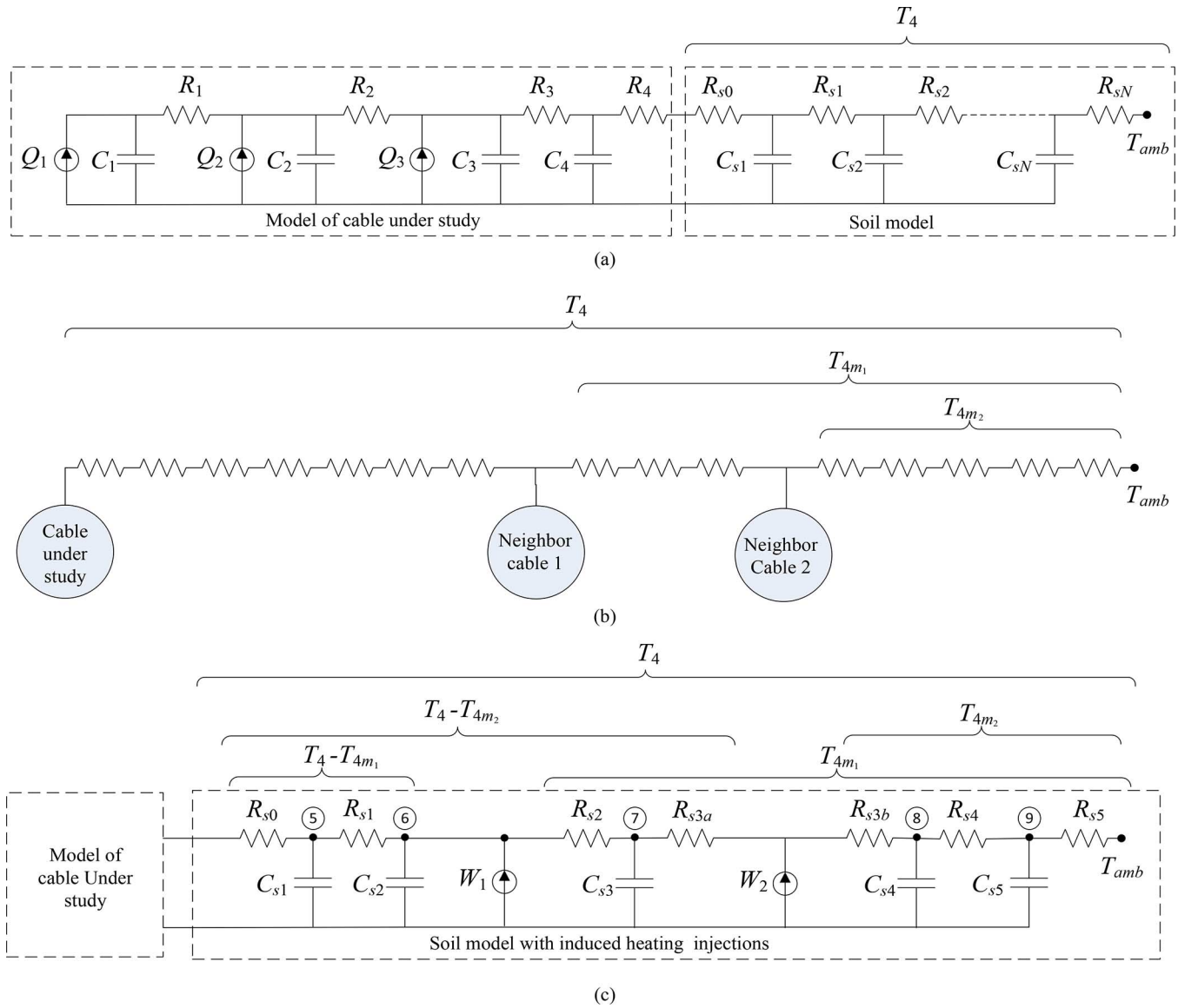

Fig. 1. Ladder-type equivalent circuit for a cable of four layers and its surrounding soil that has been discretized into five layers. Two current injections representing the losses of two neighboring cables are W_1 and W_2. (a) The cable model together with the soil model is shown. (b) The location of the injection points in the resistive model (without capacitances) is shown. (c) The complete soil model, together with the mutual heating heat sources, is shown; the model of the cable as shown in (a) is not repeated in (c), but is used for the calculations.

$\Delta\theta_{kp}$ can be seen as an equivalent T_{4m_k} resistance used to compute the effects of the mutual interactions of each of the neighboring cables (when $W_k = 1$). This mutual interaction can be computed as

$$T_{4m_k} = \frac{1}{2\pi}\rho_T \ln\left(\frac{d'_{pk}}{d_{pk}}\right). \tag{7}$$

Note that the resistance introduced in (7) is a steady-state limit of the exponential integrals, but does not introduce the loss term [2]. A similar approach to the one in (7) is presented in [18]. Therefore, the temperature rise at cable p in steady-state conditions (3) can be rewritten as

$$\Delta\theta_p = W_p T_4 + \sum_{k=1}^{N-1} W_k T_{4m_k}. \tag{8}$$

A similar rationale allows the reuse of the model defined in [22] (copied here in Fig. 1(a) for completeness), to include the mutual heating effects of all neighboring cables in a single *RC* ladder-type model for transient simulations of the cable under study (p). In this case, the losses of cable p (W_p) are the losses modeled as Q_1, Q_2, and Q_3 in Fig. 1(a), which represent the losses in the conductor, insulation, and sheath, respectively. Thus, these losses circulate through all of the resistances R_{si} in the soil model and represent the first term on the right hand in (8).

On the other hand, the losses from the other cables (W_k) need to be injected at the proper location of the *RC* soil model. Thus, the model in Fig. 1(a) can be reused if W_k is injected at a node that has a cumulative thermal resistance (cumulative resistance measured from the cable surface outwards) of $T_4 - T_{4m_k}$ [see Fig. 1(b) and (c)] by using (4) and (7), which take into account

the relative position of the cables. The losses should be injected exactly at this location to produce accurate results. If the value of $T_4 - T_{4m_k}$ falls within one of the R_{si} resistances, this resistance is split into two subresistances R_{sia} and R_{sib}, whose values are computed from the value of $T_4 - T_{4m_k}$. Then, the losses are injected at the connecting point of these two subresistances [see Fig. 1(c) for a specific example]. This is important to maintain the coherent behavior of the model in steady-state conditions. An example can be observed in Fig. 1(c), where the first injection point coincides with the resistances of the first two nodes of the soil model but the second injection point lies within the resistance R_{s_3}; therefore, this resistance is split into two subresistances ($R_{s3} = R_{s3a} + R_{s3b}$) that are computed from $T_4 - T_{4m_2}$. This modeling approach is based on the principle of superposition; thus, it can be easily extrapolated to work with any number of neighboring cables N. To do so, one needs to compute a different injection for each of the neighboring cables.

Note that the injection point depends only on the value of the steady-state resistances T_4 and T_{4m_k}, and since these resistances are defined by the relative location of the cables, the injection point is determined by the geometry of the installation. This is reasonable, because the mutual heating effects will depend mainly on the geometry (modeled by the injection point), the losses in the cable (modeled by W_k), and by the characteristics of the soil (modeled in the *RC* ladder-type model in [22]).

This model enables the possibility of computing the mutual heating effects in steady-state and transient conditions avoiding the solution of involved exponential integral equations and preserving the layered modeling presented in the standards. This feature permits using all of the widely available techniques for the analysis of electrical circuits. Also, this modeling can be directly translated into state-space equations, which are extensively used in the study of dynamical systems and solve the dynamical equations by any adequate integration method, such as Runge Kutta methods.

IV. Results

This section demonstrates that the model presented in the previous section delivers accurate results for different types of scenarios. The cable used to conduct all of these analyses is depicted in Fig. 2. Note, however, that the cable itself and the model of the cable are not the subject of this paper. The techniques presented in the paper are valid for any cable.

The first case study (although it is unrealistic, it is used to illustrate the method) consists of two cables buried at 1 m, running in parallel with a separation of 25 cm and carrying 1000 A; the geometry of this installation is illustrated in Fig. 3. With a current of 1000 A, the cables reach a steady-state temperature of 97°C. However, when the two cables are separated by 100 cm, they reach a temperature of 80 °C. All available ampacity calculation tools agree with these steady-state results, that is, the model presented before, the IEC standard [3], and finite-element simulations all report 97 °C and 80 °C, respectively.

When these same case studies are analyzed in transient conditions, for example, Cable 1 is carrying 1200 A for 168 h and Cable 2 is carrying 600 A for 48 h and 1500 A for the remaining 120 h, the model proposed in Section III produces very accurate results matching the results obtained by finite-element simulations. Figs. 4 and 5 compare the results of FEM simulations with the model for both case studies. In Fig. 4, the cables are 25 cm apart and in Fig. 5, they are 100 cm apart. As can be observed, the model reproduces accurately the thermal transient evolution that is computed by the finite-element simulations in both studies. Fig. 3 shows a snapshot of the thermal distribution at the last instant of this transient simulation, that is, at $t = 168$ h, for the simulation shown in Fig. 4.

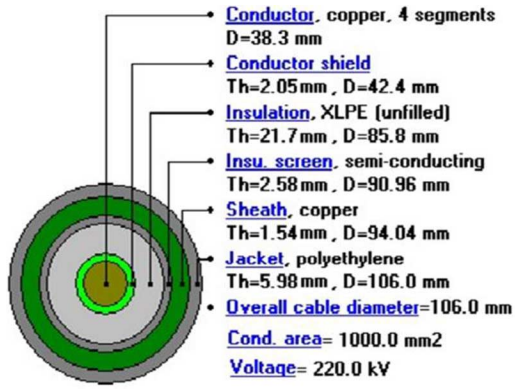

Fig. 2. Model of the cable used in the examples of this paper. The cable has six layers: copper conductor, screen, XLPE insulation, screen, copper sheath, and PE jacket. The cross-sectional area of the cable is 1000 mm^2, maximum-allowable conductor temperature for continuous operation is 90°C, and its voltage rating is 220 kV. A single cable at 1 m within a soil of resistivity of 0.9 k W/m has a steady-state ampacity of 1145 A.

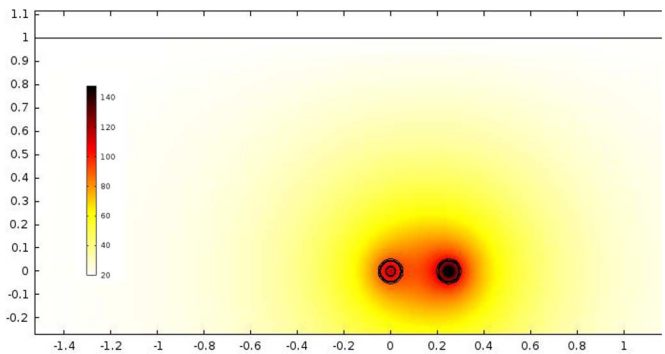

Fig. 3. Thermal 2-D illustration of the temperature distribution of two single phase cables buried in soil at 1 m and with a separation of 25 cm.

In the first case, when the cables are only 25 cm apart, it is interesting to note that Cable 1 experiences an increase of the first temperature derivative four-and-a-half hours after the neighboring cable experiences a step of current from 600 up to 1500 A. The step of current occurs at t = 48 h, but the effects are perceived by Cable 1 at t = 52.5 h. This is correctly captured by the mutual heating model. Nevertheless, in the case study where the cables are 100 cm apart, this sudden mutual heating effect is not that relevant.

Further verification has been done with other case studies, where two three-phase flat formations or trefoil formations are running in parallel at 1 m depth. The geometry corresponding to a case study of two flat formations' installation can be observed in Fig. 6 and the results are plotted in Fig. 7. Note that in these cases, the total number of cables under analysis is 6.

In Fig. 7, one can see that the thermal evolution of each individual cable computed by the model (in colors and thick lines)

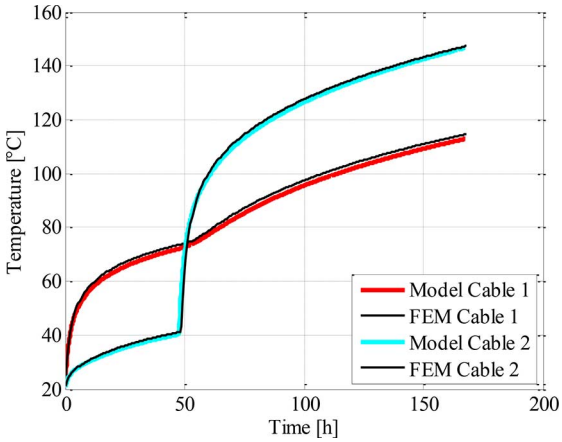

Fig. 4. Transient thermal simulation of two cables placed at 1 m depth with a separation of 25 cm. Cable 1 is carrying 1200 A for 168 h and Cable 2 is carrying 600 A for 48 h and 1500 A for the remaining 120 h.

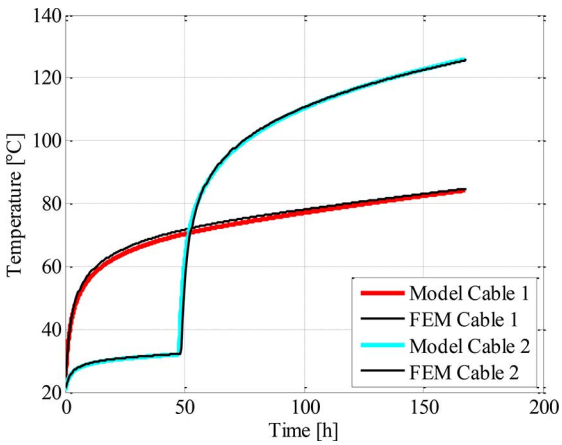

Fig. 5. Transient thermal simulation of two cables placed at 1 m depth with a separation of 100 cm. Cable 1 is carrying 1200 A for 168 h and Cable 2 is carrying 600 A for 48 h and 1500 A for the remaining 120 h.

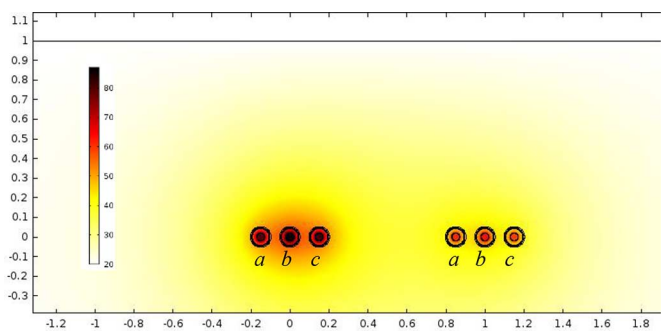

Fig. 6. Thermal 2-D illustration of the temperature distribution of two flat formation cable installations buried in soil at 1 m. The formations are separated by 100 cm and the distance between cables is 15 cm. The results show the temperature distribution at the final instant ($t = 168$ h) of the simulation described in Section IV.

is nearly identical to the thermal evolution computed by the finite-element simulations (black and thin lines). In this figure, it is important to note that due to the proximity of the two three-phase cables, the two phases that are closer together will experience relevant mutual heating effects (i.e., phase c from

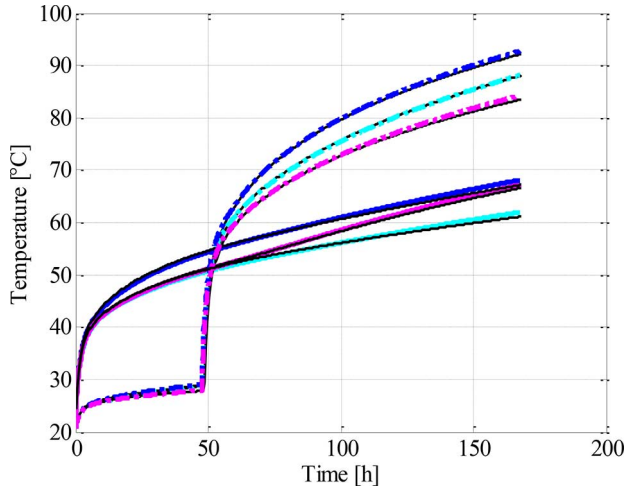

Fig. 7. Transient thermal simulation of two three-phase flat formation cables placed at 1-m depth with a separation of 100 cm. Cable 1 (dashed lines) is carrying 600 A for 48 h and 1500 A for the remaining 120 h and Cable 2 (solid lines) is carrying 1200 A for 168 h. The separation between the phases of each formation is 25 cm.

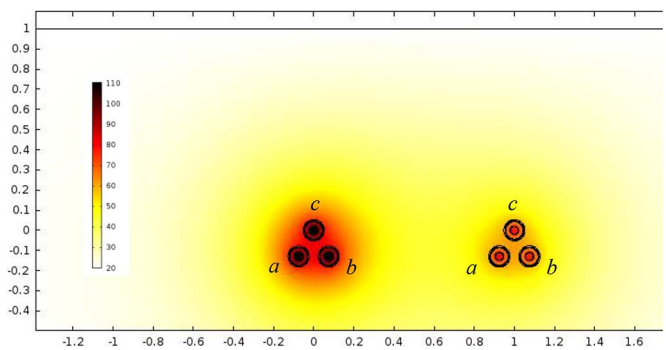

Fig. 8. Thermal 2-D illustration of the temperature distribution of two trefoil formation cable installations buried in soil at 1 m. The formations are separated by 100 cm and the distance between cables is 15 cm. The results show the temperature distribution at the final instant ($t = 168$ h) of the simulation described in Section IV. The phases of the three-phase cable are specified in the figure.

Cable 1 and phase a from Cable 2; see Fig. 6). Thus, in the case study of Fig. 7, the lagging phase (a) (in the pink and solid thick trace) of Cable 2 experiences more heat from the other cable when the step current is applied to Cable 1 than the leading phase (c) (in light blue color and solid trace). Thus, the lagging phase (a) starts heating up faster than the leading phase (c). Note that this inverts the normal behavior for this flat configuration where the leading phase (c) always runs hotter than the lagging phase (a). For instance, this behavior is the one observed for Cable 1. After 48 h, the difference is of more than 8 °C, showing that these effects can lead to important temperature differences in some situations.

To assess the performance of the mutual heating model in different scenarios, we have conducted a sensitivity analysis by varying several parameters in the installations. The parameters varied in the study are the resistivity of the soil, the heat capacity of the soil, soil density, the separation of the formations, and the separation between the phases of the three-phase cables. All of these parameters have been swept individually and we have computed the maximum mismatch between the results provided

TABLE I
SENSITIVITY ANALYSIS OF THE ACCURACY OF THE MUTUAL HEATING MODEL FOR THE FLAT FORMATION CASE

Type soil characteristic	Distance between formations [cm]	Distance between phases [cm]	Mismatch [%]
Type I	100	15	1.98
Type II	100	15	2.36
Type III	100	15	3.01
Type I	200	15	0.34
Type II	200	15	0.39
Type III	200	15	1.03
Type I	100	25	0.38
Type II	100	25	0.39
Type III	100	25	0.59
Type I	200	25	0.43
Type II	200	25	0.38
Type III	200	25	0.76

TABLE II
SENSITIVITY ANALYSIS OF THE ACCURACY OF THE MUTUAL HEATING MODEL FOR THE TREFOIL FORMATION CASE

Type soil characteristic	Distance between formations [cm]	Distance between phases [cm]	Mismatch [%]
Type I	100	15	0.65
Type II	100	15	0.84
Type III	100	15	2.17
Type I	200	15	0.63
Type II	200	15	0.74
Type III	200	15	1.90
Type I	100	25	0.92
Type II	100	25	1.19
Type III	100	25	1.80
Type I	200	25	0.85
Type II	200	25	1.18
Type III	200	25	1.90

by the finite-element computations and the simulations provided by the mutual heating model.

The results of this sensitivity analysis are listed in Tables I and II. In these tables, three types of soils are tested. Their characteristics are as follows:

Type I: $\rho = 0.5$ m K/W, $C_p = 2100$ J/kg K, $Den = 1300$ kg/m^3

Type II: $\rho = 0.9$ m K/W, $C_p = 1970$ J/kg K, $Den = 1107$ kg/m^3

Type III: $\rho = 2.5$ m K/W, $C_p = 1800$ J/kg K, $Den = 900$ kg/m^3

where ρ is the resistivity of the soil, C_p is the heat capacity, and *Den* stands for its density.

One can observe that the model behaves correctly in all of these scenarios. Also, when the distance between the cables or between each phase is varied, the relative mismatch is always below 3.01%.

V. CONCLUSION

This paper has proposed an enhancement to the *RC* thermal equivalent ladder model for the calculation of the transient mutual heating effects in underground cable installations. The model produces very accurate results in different scenarios and it is perfectly compatible with the electrothermal models used in the standards for steady-state calculations. This modeling approach complements the available set of tools to produce accurate and reliable real-time thermal computations that now rely on the solution of exponential integral equations.

The model of this paper has been extensively validated against finite-element simulations with varied realistic cable installations.

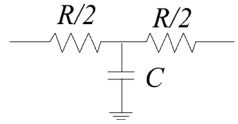

Fig. 9. Equivalent electrothermal circuit (T-equivalent circuit) used in each layers in the *RC* ladder-type model presented in [22].

APPENDIX A
LADDER-TYPE SOIL MODEL

This Appendix is devoted to summarize the *RC*-ladder type soil model used throughout this paper. The material has been summarized from [22].

It is proposed that the soil surrounding cables should be subdivided into several concentric layers. Each soil layer is modeled with its *RC* thermal T-equivalent circuit (see [22, Fig. 9]). In this way, the soil model is compatible with the cable model of the IEC standards [2], [3]. The characteristics of each soil layer are computed from the thermal resistivity, the heat capacity of the soil, and the dimensions of each layer as follows:

$$R = \frac{\rho}{2\pi} \log\left(1 + \frac{th}{r_{\text{int}}}\right) \tag{9}$$

$$C = \pi(r_{\text{ext}}^2 - r_{\text{int}}^2) \cdot C_p. \tag{10}$$

This formulation is applicable to hollow cylindrical shapes [2]. In these expressions, ρ is the thermal resistivity; th is the thickness of the layer; r_{ext} and r_{int} stand for the layer external radius and internal radius, respectively; and C_p is the heat capacity of the soil material.

As discussed in [22], several thin layers near the cable are necessary to capture the fast heat-transfer transients, and thicker layers can be used in the far region of the soil since they represent the slow transients. In [22], an optimization procedure to find the proper distribution of layers that produce the best modeling accuracy for a wide range of realistic installations was used. Specifically, the model is optimized for several transient durations: 1 h, 24 h, 168 h (1 week), and 720 h (1 month); for different burial depths: 0.5, 1.3, 2.2, 3, 6, 10, and 15 m; and for different thermal resistivities (from 0.5 to 4 k W/m) of the soil. Thus, the obtained model works for the great majority of real-world installations and can be used as a generic optimal model.

The result of such optimization leads to a model where the soil layers are distributed following an exponential discretization with the following expression:

$$b_i = r_c + (d_m - r_c) \cdot \frac{e^{\gamma \cdot i} - 1}{e^{\gamma \cdot N} - 1} \tag{11}$$

where b_i are the radial positions of the layer borders, N is the number of layers of the discretization, r_c is the radius of the cable, and d_m is the depth of the model. Finally, $i = 0, 1, \ldots N$ represents the index of the layer. Therefore, there are $N + 1$ divisions, which correspond to N layers in the model. To ensure the correct behavior of the model in steady state, the depth of the model d_m needs to be equal to [22]

$$d_m = L + \sqrt{L^2 - r_c^2}. \tag{12}$$

γ is the argument of the exponential distribution, and optimum results are obtained for $\gamma = 1.32$ when it is combined with a model of only five layers ($N = 5$). This model performs with an average accuracy of 0.44 °C across all scenarios.

In order to construct the soil *RC* model, all of the dimensions of the soil layers should be computed using (11). Then, all of the resistances and capacitances of each layer need to be computed using (9) and (10). Finally, all layers of the model [22, Fig. 9] should be concatenated by adding the corresponding resistances that lie connected in series to obtain the full soil model that is represented in Fig. 1(a).

REFERENCES

[1] F. de León, "Major factors affecting cable ampacity," presented at the IEEE Power Eng. Soc. Gen. Meeting, Montreal, QC, Canada, 2006.

[2] G. J. Anders, *Rating of Electric Power Cables*. New York, USA: McGraw-Hill, 1997.

[3] *Calculation of the Current Ratings*, IEC Standard 60287-1, 2001.

[4] *IEEE Standard Power Cable Ampacity Tables*, IEEE Standard 835-1994, 1994.

[5] *Calculation of the Cyclic and Emergency Rating of Cables*, IEC Standards 60853-1 and 60853-2, 1989.

[6] M. Matus, D. Saez, M. Favley, C. Suazo-Martinez, J. Moya, G. Jimenez-Estevez, R. Palma-Behnke, G. Olguin, and P. Jorquera, "Identification of critical spans for monitoring systems in dynamic thermal rating," *IEEE Trans. Power Del.*, vol. 27, no. 2, pp. 1002–1009, Apr. 2012.

[7] S.-H. Huang, W.-J. Lee, and M.-T. Kuo, "An online dynamic cable rating system for an industrial power plant in the restructured electric market," *IEEE Trans. Ind. Appl.*, vol. 43, no. 6, pp. 1449–1458, Nov. 2007.

[8] G. J. Anders, A. Napieralski, M. Zubert, and M. Orlikowski, "Advanced modeling techniques for dynamic feeder rating systems," *IEEE Trans. Ind. Appl.*, vol. 39, no. 3, pp. 619–626, May 2003.

[9] S. P. Walldorf, J. S. Engelhardt, and F. J. Hoppe, "The use of real-time monitoring and dynamic ratings for power delivery systems and the implications for dielectric materials," *IEEE Elect. Insul. Mag.*, vol. 15, no. 5, pp. 28–33, Oct. 1999.

[10] T. H. Dubaniewicz, P. G. Kovalchik, W. L. Scott, and M. A. Fuller, "Distributed measurement of conductor temperatures in mine trailing cables using fiber-optic technology," *IEEE Trans. Ind. Appl.*, vol. 34, no. 2, pp. 395–398, Apr. 1998.

[11] D. A. Douglass, A. Edris, and G. A. Pritchard, "Field application of a dynamic thermal circuit rating method," *IEEE Trans. Power Del.*, vol. 12, no. 2, pp. 823–831, Apr. 1997.

[12] D. A. Douglass and A. Edris, "Real-time monitoring and dynamic thermal rating of power transmission circuits," *IEEE Trans. Power Del.*, vol. 11, no. 3, pp. 1407–1418, Jul. 1996.

[13] G. Z. Ben-Yaacov and J. G. Bohn, "Methodology for real-time calculation of temperature rise and dynamic ratings for distribution system duct banks," *IEEE Trans. Power App. Syst.*, vol. PAS-101, no. 12, pp. 4604–4610, Dec. 1982.

[14] CIGRE Working Group 21.02, "Computer method for the calculation of the response of single core cables to a step function thermal transient," *Electra*, vol. 87, pp. 41–64, Mar. 1985.

[15] G. Mazzanti, "Analysis of the combined effects of load cycling, thermal transients, and electrothermal stress on life expectancy of high-voltage AC cables," *IEEE Trans. Power Del.*, vol. 22, no. 4, pp. 2000–2009, Oct. 2007.

[16] G. Mazzanti and M. Marzinotto, "More insight into the effects of load cycles and electrothermal stress on HVDC extruded cable reliability in the prequalification test," in *Proc. IEEE Power Energy Soc. Gen. Meeting*, 2013, pp. 1–5.

[17] M. Diaz-Aguilo and F. de León, "Adaptive soil model for real-time thermal rating of underground power cables," *IET Sci. Meas. Technol.*, 2014, accepted for publication.

[18] E. Tarasiewlcz, M. A. El-Kady, and G. J. Anders, "Generalized coefficients of external thermal resistance for ampacity evaluation of underground multiple cable systems," *IEEE Trans. Power Del.*, vol. PWRD-2, no. 1, pp. 15–20, Jan. 1987.

[19] R. J. Millar and M. Lehtonen, "A robust framework for cable rating and temperature monitoring," *IEEE Trans. Power Del.*, vol. 21, no. 1, pp. 313–321, Jan. 2006.

[20] R. S. Olsen, "Dynamic loadability of cable based transmission grids," Ph.D. dissertation, Dept. Elect. Eng., Technical University of Denmark, Copenhagen, Denmark, 2013.

[21] R. Olsen, G. J. Anders, J. Holboell, and U. S. Gudmundsdottir, "Modelling of dynamic transmission cable temperature considering soil-specific heat, thermal resistivity, and precipitation," *IEEE Trans. Power Del.*, vol. 28, no. 3, pp. 1909–1917, Jul. 2013.

[22] M. Diaz-Aguilo, F. de León, S. Jazebi, and M. Terracciano, "Ladder-type soil model for dynamic thermal rating of underground power cables," *Proc. IEEE Power Energy Technol. Syst.*, vol. 1, no. 1, pp. 1–10, Dec. 2014.

[23] R. N. Patton, S. K. Kim, and R. Podmore, "Monitoring and rating of underground power cables," *IEEE Trans. Power App. Syst.*, vol. PAS-98, no. 6, pp. 2285–2293, Nov. 1979.

[24] J. H. Neher, "The temperature rise of buried cables and pipes," *AIEE Trans.*, vol. 68, no. 1, pp. 9–21, 1949.

[25] A. E. Kennelly, "Discussion of electrical congress programme," *AIEE Trans.*, vol. X, pp. 363–369, 1893.

[26] J. H. Neher and M. H. McGrath, "The calculation of the temperature rise and load capability of cable systems," *AIEE Trans. Power App Syst. Part III*, vol. 76, no. 3, pp. 752–764, 1957.

Marc Diaz-Aguiló was born in Barcelona, Spain. He received the M.Sc. degree in telecommunications engineering from the Technical University of Catalonia (UPC), Barcelona, Spain, in 2006 and the M.Sc. degree in aerospace controls engineering from a joint program between Supaero, Toulouse France, and the Massachusetts Institute of Technology, Cambridge, MA USA, in 2008, and the Ph.D. degree in aerospace simulation and controls from the Technical University of Catalonia, Barcelona, Spain, in 2011.

Currently, he is a Postdoctoral Researcher at the Polytechnic Institute of New York University, Brooklyn, NY, USA. His research interests are in power systems, controls, smart-grid implementations, and large systems modeling and simulation.

Francisco de León (S'86–M'92–SM'02–F'15) received the B.Sc. and the M.Sc. (Hons.) degrees in electrical engineering from the National Polytechnic Institute, Mexico City, Mexico, in 1983 and 1986, respectively, and the Ph.D. degree in electrical engineering from the University of Toronto, Toronto, ON, Canada, in 1992.

He has held several academic positions in Mexico and has worked for the Canadian electric industry. Since 2007, he has been an Associate Professor with the Department of Electrical and Computer Engineering at the Polytechnic School of Engineering of New York University, Brooklyn, NY, USA. His research interests include the analysis of power phenomena under nonsinusoidal conditions, the transient and steady-state analyses of power systems, the thermal rating of cables and transformers, and the calculation of electromagnetic fields applied to machine design and modeling.

Prof. de León is an Editor of the IEEE TRANSACTIONS ON POWER DELIVERY and the IEEE POWER ENGINEERING LETTERS.